IEEE Access
Multidisciplinary ⋮ Rapid Review ⋮ Open Access Journal

Received 28 March 2023, accepted 3 May 2023, date of publication 8 May 2023, date of current version 17 May 2023.

Digital Object Identifier 10.1109/ACCESS.2023.3273809

RESEARCH ARTICLE

An Adaptive Kalman Filter-Based Condition-Monitoring Technique for Induction Motors

JAEHOON KIM[1], MOOGEUN SONG[1], DONGGIL KIM[2], AND DONGIK LEE[1], (Member, IEEE)

[1]School of Electronic and Electrical Engineering, Kyungpook National University, Bukgu, Daegu 41566, South Korea
[2]Department of Robot Engineering, Kyungil University, Gyeongsan 38428, South Korea

Corresponding author: Dongik Lee (dilee@ee.knu.ac.kr)

This work was supported in part by the National Research Foundation of Korea (NRF) funded by the Korean Government (MSIT) (50%) under Grant 2018K1A3A7A03089832, and in part by the Institute of Information & Communications Technology Planning & Evaluation (IITP) funded by the Korean Government (MSIT) (50%) under Grant 2021000999.

ABSTRACT Induction motors are typical rotating machines that are widely used in various industrial processes. The condition of induction motors has to be monitored to avoid serious losses, which can be caused by various reasons. Over the last decades, although many studies have been performed on the condition monitoring (CM), there is still an increasing need for cost-effective and reliable CM techniques for induction motor. This paper presents an adaptive Kalman filter (AKF)-based CM technique for an induction motor driving a scrubber fan. In this work, AKFs are used to extract useful information about the induction motor's condition based on measured vibration signals. The main novelty of the proposed method is the use of multiple AKFs for the detection of outliers and anomalies. The output of the AKFs plays as the basis of severity assessment on the vibration signals. A set of AKFs are employed to deal with various anomaly conditions caused by different severity levels of vibration as the IM is deteriorated. Moreover, the effectiveness of the proposed method is demonstrated through experiments involving a real scrubber fan driven by an induction motor.

INDEX TERMS Adaptive Kalman filter, condition monitoring, failure detection, induction motor, severity assessment.

I. INTRODUCTION

The failure or malfunctioning of induction motors (IMs), which are core devices in industrial processes, can result in unnecessary downtimes, substantial repairs, and revenue losses. IMs are usually operated under heavy loads and high-speed conditions; thus, under these harsh conditions, even a small defect can accelerate the degradation process of IMs. To prevent severe damage and reduce unscheduled downtimes and maintenance costs, it is highly imperative to develop a condition-monitoring (CM) technology capable of detecting the failures of IMs and evaluating their health status online [1].

A variety of CM techniques have been proposed to detect faults of IMs based on various sensing technologies using vibration [2], [3], current [4], acoustic emission [5], infrared thermography [6], etc. Many authors have focused on extracting fault signatures from measured signals to detect distinct defects in the IM. Commonly used signal processing techniques include FFT, wavelet transform [7], [8], [9], Kalman filtering (KF) [10], and statistical approach [11], which are simple but require a more analytical approach. Meanwhile, various machine learning techniques, including deep learning, artificial neural networks, principal component analysis, and support vector machines, have also been widely applied in fault detection [12], [13], [14], [15], [16], [17], [18], [19], [20], [21]. One disadvantage of machine learning techniques is that their performance is highly dependent on the quality and quantity of the data to be learned. Some authors have suggested model-based fault detection approaches that rely on mathematical models of IMs [22], [23], [24], [25], [26], [27]. The primary limitation of the model-based approach for

The associate editor coordinating the review of this manuscript and approving it for publication was Pinjia Zhang.

fault detection in IMs is the unreliability of the mathematical model, which is affected by changes in the IM's parameters over time due to load levels, environmental factors, such as temperature and lubricant viscosity, and the presence of external disturbances, which can impact the accuracy of parameter estimation techniques.

Health management technology for IMs is equally important as fault diagnosis. In real-world industrial settings, there may be cases where it is not possible to immediately shut down an IM even if a fault is detected. Therefore, health management techniques are necessary to predict potential failures caused by faults that could lead to catastrophic accidents. Climente-Alarcon et al. [28] proposed a condition-based maintenance and prognostics and health management strategy based on an in-depth experimental analysis of the failure mechanism of reproduced rotor-bar breakage. Li et al. [29] suggested a fault index for quantifying the heath status of an IM and demonstrated its effectiveness for broken rotor bars and damaged bearing. In [30], a data-driven approach coupled with unscented Kalman filter is proposed to enable predictive health management for bearing. In addition to these papers, various CM methods have been reported for health management of IMs [31], [32], [33], [34], [35], [36], [37].

Aforementioned CM techniques for IMs are mostly based on detailed knowledge such as well-defined fault-related knowledge (e.g. fault type, specification data), mathematical model of induction motor with known parameters, or historical data from faulty motors which are usually realized by an artificial fault reproduction feasible only in laboratory environments. The practical application of these fault diagnosis and health management methods is usually limited to the single-type fault situations or components of induction motor. However, when performing CM at the component level of an IM, there are several drawbacks. Firstly, some faults may not have clear and unique signatures that can be identified at the component level, making it challenging to diagnose them accurately. Secondly, simultaneous occurrence of multiple faults in different components of the motor can make it challenging to isolate and identify individual faults. Finally, due to the complexity of the system, which consists of multiple components, it is impractical to apply component-level CM techniques individually on industrial induction motors. Therefore, it is necessary to develop holistic CM techniques that can analyze the motor's overall health status and predict failures at the system level. Such techniques can provide a more comprehensive understanding of the motor's health and performance, thus improving the motor's reliability, availability, and maintenability.

As far as induction motors are concerned, this paper presents a system-level approach to failure detection and health management of IMs, using Kalman filtering technique and vibration acceleration measurements. This method has the advantage of being a standalone tool and having real-time signal processing capabilities, which makes it highly useful for induction motor condition monitoring. Several studies have investigated the effectiveness of Kalman filtering-based monitoring techniques, demonstrating their potential for managing the health of IMs [38], [39], [40], [41], [42]. The proposed KF-based CM method can be easily applied in industrial site in a cost-effective and straightforward manner without the need for destructive testing, complicated sensor installation processes, historical data related to faults, or predefined knowledge of the dynamic model and fault types of an IM. The main challenges in this approach are to estimate the random vibration signals and to quantify the health status of the IM with thresholding. To address these challenges, an adaptive Kalman filter has been proposed, and multiple adaptive Kalman filters are utilized.

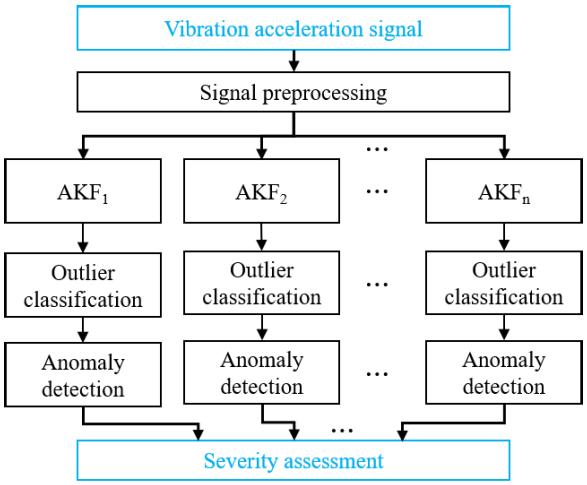

FIGURE 1. Flowchart of the proposed AKF-based CM technique.

Figure 1 shows the proposed AKF, which serves as an underlying tool for outlier detection, anomaly detection, and vibration severity assessment. The AKFs are designed with the so-called random walk model to extract failure signatures while tracking measured vibration signals and provide estimates, where each estimate is a weighted sum of prediction and measured data. The estimates of the AKF are classified into normal data and outliers through a normal hypothesis test, through which adaptive thresholds are generated online to detect outliers. Based on the classification results, anomalies could be detected. The novelty of the proposed AKF is highlighted by the property that it can be used to detect different anomaly conditions by manipulating the AKF's *a priori* knowledge about measurement uncertainty. The severity level of IM vibration can be assessed using multiple AKFs with different *a priori* knowledge about measurement uncertainty. Based on the vibration severity assessment, the health status of an IM is evaluated.

II. PRELIMINARIES

We suppose that a vibration signal changes randomly from its previous value in the discrete-time domain. In addition, if the changes are assumed to be due to additive process noise, a discrete-time stochastic model can be obtained as follows:

$$x(k+1) = x(k) + w(k), \tag{1}$$

$$y(k) = x(k) + v(k), \tag{2}$$

where $x(k)$ denotes the vibration signal, $w(k)$ is the additive process noise assumed to be zero-mean Gaussian noise with variance $Q(k)$, and $y(k)$ is the measurement (observation) subject to the measurement noise $v(k)$ assumed to be zero-mean Gaussian noise with variance $R(k)$. Based on the stochastic model defined by (1) and (2), it is possible to implement a Kalman filtering technique for the estimation of $x(k)$.

The convergence property of a standard Kalman filter depends on the noise variances $Q(k)$ and $R(k)$, which need to be given as *a priori* knowledge of noise uncertainties. Therefore, it is important for standard Kalman filters to have appropriate $Q(k)$ and $R(k)$ so as to achieve satisfactory estimation performance. However, the estimation performance can be impeded by the problem that real noise uncertainties are unknown. A real process noise uncertainty changes from moment to moment since the stochastic properties of vibrations, which contain information on the health status of an IM, change as an IM deteriorates. To address this problem, an adaptation technique is developed in this work to estimate the process noise variance $Q(k)$, and the combination of the standard Kalman filter and adaptation technique resulted in an adaptive Kalman filter (AKF).

We consider that the observation noise variance $R(k)$ is a user-defined parameter for the AKF. Thanks to the proposed adaptation technique for estimating $Q(k)$, the estimation performance of the AKF could be tuned in advance by manipulating the observation noise variance $R(k)$. Moreover, as previously mentioned, the estimation performance is closely related to the estimation of $Q(k)$, which can vary with the severity level of vibration. If an AKF with a constant $R(k)$ experiences a significant severe process noise uncertainty despite the aid of the adaptation technique and thus begins to output more than a certain number of abnormal estimates (outliers) within a certain period of time from a certain moment, it can be understood that an IM is deteriorated more than before. The multiple AKFs shown in Figure 1 have different values for $R(k)$, and they are employed to evaluate different health conditions of the IM.

III. METHODOLOGY

A. ADAPTIVE KALMAN FILTER FOR SIGNAL PROCESSING

The proposed AKF is a recursive algorithm that consists of three phases: the time update phase of the standard Kalman filter, the measurement update phase of the standard Kalman filter, and the adaptation phase for the estimation of $Q(k)$. For step k, we denote the estimate and its error variance by $\hat{x}^-(k)$ and $P^-(k)$ after the time update phase and by $\hat{x}(k)$ and $P(k)$ after the measurement update phase, respectively. Considering the random process model (1), the time update equations are simply described as follows:

$$\hat{x}^-(k) = \hat{x}(k-1), \tag{3}$$
$$P^-(k) = P(k-1) + \hat{Q}(k-1). \tag{4}$$

The time update phase is combined with the measurement update phase, which is formulated as follows:

$$\tilde{y}(k) = y(k) - \hat{x}^-(k), \tag{5}$$
$$Y(k) = P^-(k) + R(k), \tag{6}$$
$$K(k) = P^-(k)Y^{-1}(k), \tag{7}$$
$$\hat{x}(k) = \hat{x}^-(k) + K(k)\tilde{y}(k), \tag{8}$$
$$P(k) = (1 - K(k))P^-(k), \tag{9}$$

where $\tilde{y}(k)$ is the innovation, $Y(k)$ is the innovation variance, and $K(k)$ is the Kalman gain.

In (4), the process noise variance used for the time update of the error variance is the estimate calculated in the previous step. To make this time update law applicable for every step k, the recursive AKF additionally includes the adaptation phase providing $\hat{Q}(k)$ to be used in the next step $k+1$ in the following form:

$$\hat{Q}(k) = S(k)M(k), \tag{10}$$

where $M(k)$ is a residual variance and $S(k)$ is a scaling factor.

Without loss of generality, we assume that the residual sequence, $y(k) - \hat{x}(k)$, is normally distributed with zero mean. Then, the residual variance can be approximately calculated using samples within a sliding window of size N:

$$M(k) = \frac{1}{N}\sum_{j=j_0}^{k}(y(j) - \hat{x}(j))^2, \tag{11}$$

where $j_0 = k - N + 1$. In our setup, where $\hat{Q}(k)$ is positively correlated with $M(k)$, the estimate $\hat{Q}(k)$ can be regulated by the Kalman filtering process. For instance, if $\hat{Q}(k-1)$ is increased (decreased), the Kalman filter increases (decreases) the weight for the observation, which decreases (increases) the residual variance $M(k)$ so that $\hat{Q}(k)$ decreases (increases).

Similar to the scaling law used in [43], the scaling factor can be introduced as follows:

$$S(k) = \max\left(1, \frac{\hat{G}(k)}{\tilde{G}(k)}\right), \tag{12}$$

where $\tilde{G}(k)$ is a filter-computed variance and $\hat{G}(k)$ is a numerically calculated variance. These variances can be derived from the following assumptions. In a steady-state condition, i) the Kalman gain $K(k)$ is constant and ii) the innovation $\tilde{y}(k)$ is a zero-mean Gaussian random variable. If we denote the correction component $\hat{x}(k) - \hat{x}^-(k)$ by $\Delta\hat{x}(k)$ based on evidence from (8), it can be seen that $\Delta\hat{x}(k)$ is also a zero-mean Gaussian random variable with a variance $G(k)$ since $\mathrm{E}[\Delta\hat{x}(k)] = \mathrm{E}[K(k)\tilde{y}(k)] = K(k)\mathrm{E}[\tilde{y}(k)] = 0$ under the assumptions i) and ii). Using the variance properties, it can be seen that $G(k) = \mathrm{Var}(\Delta\hat{x}(k)) = \mathrm{E}[\Delta\hat{x}^2(k)] = K^2(k)\mathrm{E}[\tilde{y}^2(k)]$. Considering the relation $Y(k) = \mathrm{E}[\tilde{y}^2(k)]$, the variance $G(k)$ can be approximated as a function of filter-computed variables as follows:

$$\tilde{G}(k) = K^2(k)Y(k). \tag{13}$$

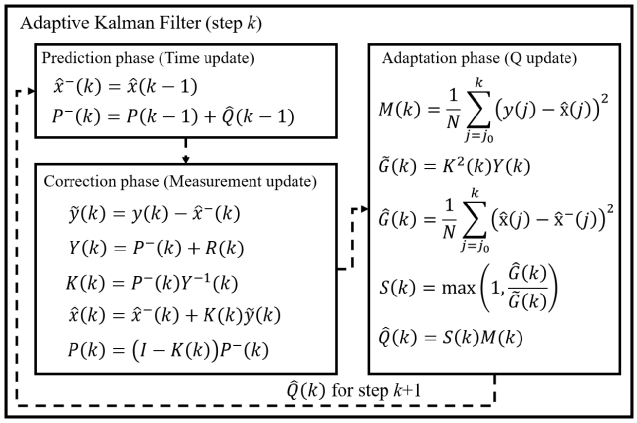

FIGURE 2. Recursive algorithm of the AKF.

Moreover, the variance $G(k)$ can be approximately calculated using recent N samples as follows:

$$\hat{G}(k) = \frac{1}{N}\sum_{j=j_0}^{k}(\Delta\hat{x}(j))^2. \tag{14}$$

As (12) shows, the scaling factor $S(k)$ to be enforced for $M(k)$ is greater than or equal to 1. If $S(k) > 1$, a fading effect is created on old data, which can improve the convergence property of the AKF [44]. Finally, the recursive algorithm of the AKF can be illustrated as shown in Figure 2.

B. OUTLIER DETECTION

An effective method for detecting outliers in the estimates of the AKF is to check the goodness of fit to the normal hypothesis that the estimation errors are normally distributed with zero mean. If a normalized random variable for the estimation error can be obtained, then it is a natural procedure for establishing a probabilistic criterion to obtain confidence intervals, which can be used to detect outliers.

Recall that the correction component $\Delta\hat{x}(k)$ is assumed to be a zero-mean Gaussian random variable with variance $G(k)$ for the steady-state filter and that the variance $G(k)$ is approximately given as $\tilde{G}(k)$. We could define a random variable $z(k)$, which is expected to be a standard normal random variable as follows:

$$z(k) = \frac{\Delta\hat{x}(k)}{\sqrt{\tilde{G}(k)}} = \frac{\Delta\hat{x}(k)}{\sqrt{K^2(k)Y(k)}}. \tag{15}$$

An outlier is detected if the condition $|z(k)| > z_c$ is satisfied, where z_c is the critical value determined based on the desired level of confidence for the standard normal random variable $z(k)$. This condition results in the detection of an outlier when the estimate $\hat{x}(k)$ deviates from the confidence interval specified by the boundaries $\hat{x}^-(k) \pm z_c\sqrt{K^2(k)Y(k)}$. Excluding the statistics that are updated by the Kalman filter itself, the variables that affect the confidence interval, which serves as a criterion for outlier detection, are the critical value z_c and the observation noise noise variance $R(k)$. In this study, the critical value is a controlled variable that remains fixed.

Note that in terms of the observation data $y(k)$, the range of the confidence interval is specified by the boundaries $\hat{x}^-(k) \pm z_c\sqrt{Y(k)}$, as the random variable $z(k)$ can be rewritten as $z(k) = \tilde{y}(k)/\sqrt{Y(k)}$ based on the relation $\Delta\hat{x}(k) = K(k)\tilde{y}(k)$. Based on (6), it is clear that a larger $R(k)$ can result in a wider range of the confidence interval. In other words, for the same vibration signal, the AKF has a characteristic of outputting a smaller number of outliers as it takes a larger $R(k)$.

The proposed outlier detection method designed with the AKF can be less affected by electromagnetic noise since it uses adaptive thresholds (i.e., confidence interval), which is effective for reducing the number of false outliers compared with conventional outlier detection methods, which use fixed thresholds.

C. ANOMALY DETECTION

Anomaly is herein defined as the condition in which an AKF with a constant $R(k)$ outputs more than a certain number of abnormal estimates (outliers) within a certain period of time. In this study, an anomaly is detected when the number of outliers per second exceeds the rotating frequency of the IM for the first time. Observation data is generated at 100 Hz. Figure 3 shows a detailed algorithm for anomaly detection, where f_r is the rotation frequency, cnt is a variable to count outliers, and F_a is a flag variable that indicates whether an anomaly is detected. At the starting point, both cnt and F_a are initialized to 0.

When a certain amount of raw data is collected, it is used to calculate an observation, which is generally the root mean square. The observation is the input to the AKF which produces various data, including the estimate $\hat{x}(k)$, so that the normalized random variable $z(k)$ can be obtained. The next step is the outlier classification, where the value of cnt is incremented by 1 only if the condition $|z(k)| > z_c$ is satisfied or otherwise it is kept as the previous value. Considering that the observations are generated every 0.01 s, it can be seen that the procedure from the data collection to the outlier classification is performed 100 times per second.

The decision-making process for anomaly detection is designed to occur at 1-s intervals. When the time comes to make a decision for the anomaly detection, the count variable cnt and rotating frequency f_r are compared. If $cnt \geq f_r$, the flag variable as F_a is set to 1 to indicate that an anomaly has been detected. If not, the following condition is evaluated: $cnt < c \cdot f_r$. When this condition is not satisfied, the value of F_a is maintained at its previous value. However, if the condition is satisfied, the flag variable F_a is set to 0, meaning either that no anomaly has been detected or that the decision made earlier that an anomaly was detected is canceled. The parameter c, which satisfies $0 < c < 1$, is introduced to cancel the previous decision that an anomaly was detected, and its value is obtained empirically. At the end of decision-making, the count variable cnt is cleared to 0 and the whole process is repeated based on new raw data.

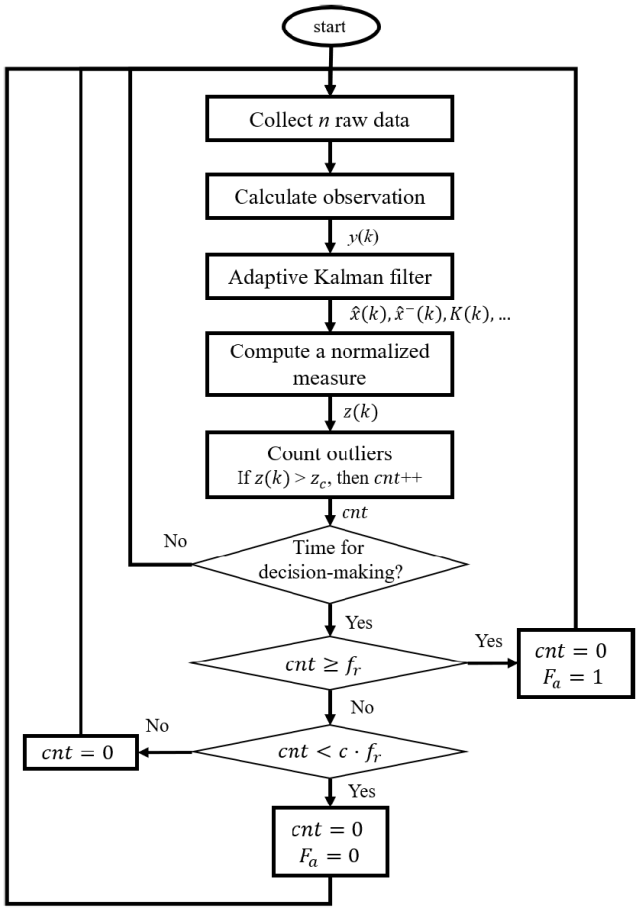

FIGURE 3. Algorithm for anomaly detection.

D. SEVERITY ASSESSMENT

To evaluate the health condition of an IM, multiple AKFs are used. For n AKFs, the ith AKF, denoted by AKF_i, has the following measurement noise variance:

$$R_i(k) = R_{min} + i\frac{R_{max} - R_{min}}{n} \quad \text{for } i = 1, \ldots, n. \tag{16}$$

where R_{min} and R_{max} are the minimum and maximum values of an acceptable range for $R(k)$, respectively. The range can be defined by examining the vibration signals of the healthy motor and faulty motor.

Recall that the larger the $R(k)$ value of AKF, the smaller the number of outliers. Therefore, the larger $R(k)$, the AKF can be used to detect more severe anomaly conditions. Based on this characteristic of AKF, the severity index can be introduced as follows:

$$S_{idx} = \max(I_1, \ldots, I_n), \tag{17}$$

where S_{idx} is the severity index and I_i for $i = 1, \ldots, n$ is an indicator representing the severity level. For AKF_i, the indicator I_i is defined as follows:

$$I_i = \begin{cases} \dfrac{i}{n}, & \text{if } F_a \text{ for } \text{AKF}_i \text{ is 1.} \\ 0, & \text{if } F_a \text{ for } \text{AKF}_i \text{ is 0.} \end{cases} \tag{18}$$

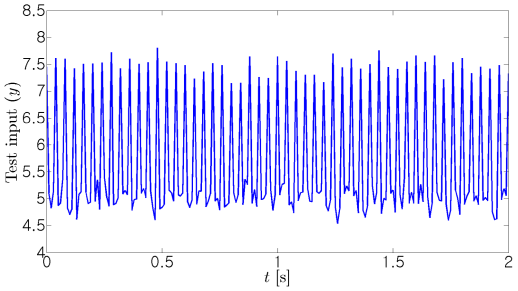

FIGURE 4. Test input for investigating the performance of the proposed AKF.

E. ILLUSTRATIVE EXAMPLE

As shown in this section, the AKF is compared with a conventional Kalman filter (KF) to illustrate the effect of the proposed adaptation technique on Kalman filtering. All the considered Kalman filters are examined under the same conditions except for $Q(k)$. As shown in Figure 4, the test input to the Kalman filters is a signal where 25 spikes per second are observed in a random signal. The sampling rate is 100 Hz, and the measurement noise variance is set to $R(k) = 10^{-2}$.

Figure 5 shows the number of outliers counted during each second. With the proposed AKF, as expected, 25 spike signals per second are detected as outliers, except for the first 1-s interval, in which the AKF is in a transient state. If the scaling factor is not applied by setting $S(k) = 1$ for all step k, twice as many outliers as the result of applying the scaling factor are detected (see the result of AKF without scaling after 1 s). This is because a single spike signal causes two large changes in the test input: when the spike signal appears and when it disappears. It can be seen from the results of conventional KFs that it is extremely difficult to search for *a priori* knowledge $Q(k)$ to obtain a consequence that classifies spikes as outliers. Wrong knowledge of $Q(k)$ can result in false outliers or in a failure to detect spike signals.

At step k, if the spike signal is input to the AKF, the residual error and its variance $M(k)$ increase so that $\hat{Q}(k)$ also increases. Then, for step $k+1$, the increased $\hat{Q}(k)$ causes an increase in the dependence of the AKF on the observations, leading to a decrease in the residual error. The scaling factor enhances the increase of $M(k)$ so that the residual error can be reduced more quickly. Consequently, the use of the estimated $\hat{Q}(k)$ results in a reduced number of false outliers. Figure 6 clearly shows the effectiveness of the adaptation technique for $Q(k)$ discussed above in comparison with other Kalman filters. The proposed AKF could reduce the residual error increased due to the spike signal at a step k to almost zero at the next step $k+1$.

IV. ENGINEERING TEST

The proposed AKF-based CM method is verified through an experiment with two industrial scrubber fan systems, as illustrated in Figure 7. One scrubber fan system is a faulty system with a deteriorated IM that requires maintenance, and the other is a healthy system. The faulty system used

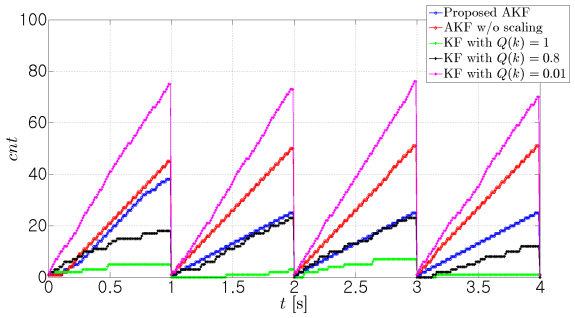

FIGURE 5. Number of outliers: the variable *cnt* is reset to 0 every second.

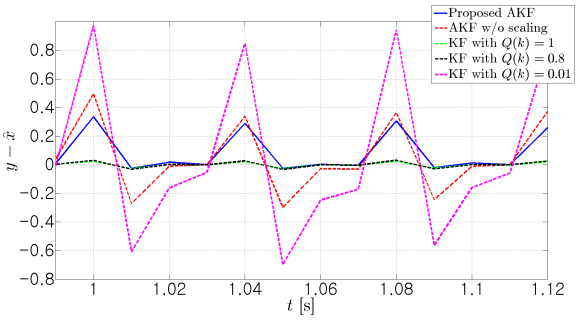

FIGURE 6. Residuals of different Kalman filters.

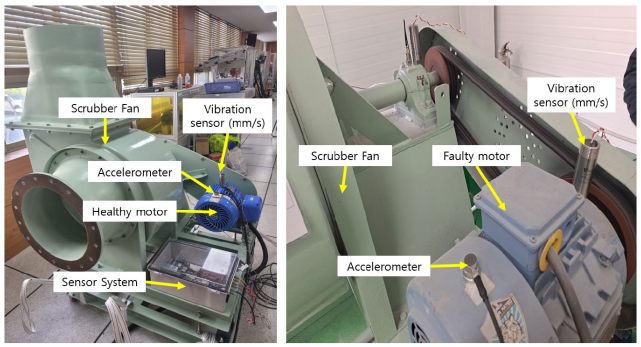

FIGURE 7. Healthy and faulty scrubber fan systems.

in the experiment is a system classified as ''UNACCEPTABLE'' because the root-mean squared vibration velocity (measured in mm/s) of the induction motor in the Z-axis exceeds 7.1 mm/s, as per the ISO 10816 standard. The classification of a faulty industrial scrubber fan according to the ISO 10816 standard provides important context and motivation for the proposed monitoring method based on adaptive Kalman filtering technique. Both systems are driven by 3-phase, 4-pole, 3.7 kW IMs. The motors run at approximately 1720 rpm; hence $f_r = 28.66$. To investigate the health status of the IMs, the accelerometers(VS-JV10A) are vertically mounted on the top of them. The developed sensor system for data acquisition consists of a sensor interface, an ADC board(EK-TM4C1294XL), a single-board computer(OdroidN2+), a switched mode power supply. Figure 8 shows the sensor system.

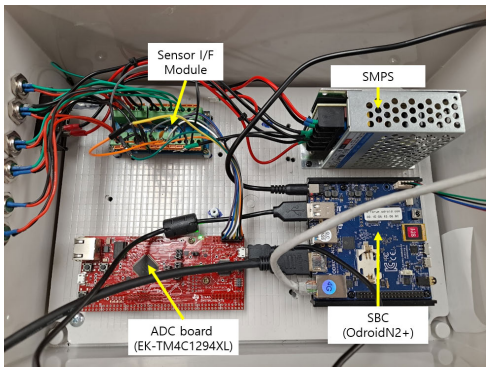

FIGURE 8. Sensor system for condition monitoring.

The analog signal of the accelerometers is sampled at 25 kHz on the ADC board through the sensor interface. The observation data of 100 Hz, which is a root mean square of 250 samples of raw data, is immediately transferred upon generation from the ADC board to the single-board computer by UART serial communication. The main algorithms, including the AKF, outlier classification, anomaly detection, and severity assessment, are written in Python and run on the single board computer (with a Linux operating system). The criterion value considered for outlier classification is $z_c = 2.8$, which corresponds to 99.5% confidence level of the standard normal distribution. As previously mentioned, the time interval for decision-making is set to 1 s.

For the sake of convenience, let us denote the *cnt* value at the decision point as cnt'. The parameter c can be obtained as $c = cnt'_{min}/cnt'_{max}$ by considering the maximum (cnt'_{max}) and minimum (cnt'_{min}) values of cnt' dataset that lie at the boundary between normal and abnormal, as shown in Figure 9 (blue graph) and Figure 10 (red graph). This method is relatively deterministic. It is advisable to find a cnt' dataset that is almost equal to or slightly larger than f_r for cnt'_{max}. Such dataset can be obtained by adjusting $R(k)$. If cnt'_{max} is assumed to be equal to f_r, then the condition $cnt < c \cdot f_r$ in Figure 3 is equivalent to $cnt < cnt'_{min}$, which means that after the first detection of anomaly, the decision is maintained until the condition $cnt < cnt'_{min}$ is satisfied. However, reversing the decision of previous anomaly detection requires more caution, so we set the value of $c = 0.4$ to be more conservative, i.e., smaller, than the observed ratio in the blue graph in Figure 9 and the red graph in Figure 10.

As shown in Figures 9 and 10, the number of outliers tends to decrease as $R(k)$ increases. Since no anomaly should be detected for the healthy motor, it is reasonable to set $R(k)$ to greater than $4 \cdot 10^{-3}$. However, for the faulty motor, it is necessary to set $R(k)$ to less than $1.3 \cdot 10^{-1}$ so that anomalies can be detected. Therefore, $R_{min} = 4 \cdot 10^{-3}$ and $R_{max} = 1.3 \cdot 10^{-1}$. In this study, the number of AKFs used to diagnose the condition of the IM is 10. If the AKF with R_{max} detects an anomaly, it is considered that the motor has failed. Figures 11 and 12 show the estimation results for the healthy motor and faulty motor, respectively. As shown in the figures, most

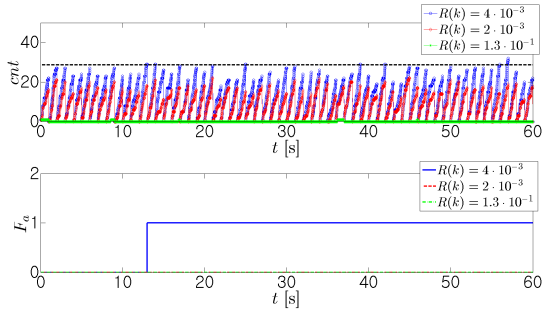

FIGURE 9. Outlier and anomaly detection results of the healthy motor.

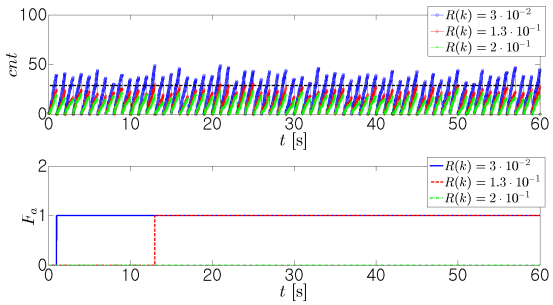

FIGURE 10. Outlier and anomaly detection results of the faulty motor.

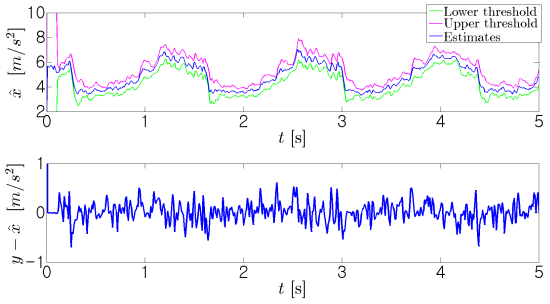

FIGURE 11. Estimation results of AKF with $R(k) = 1.3 \cdot 10^{-1}$ for the healthy motor.

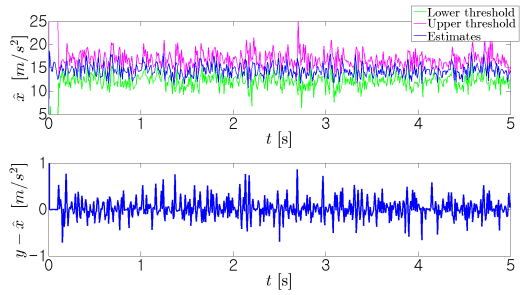

FIGURE 12. Estimation results of AKF with $R(k) = 1.3 \cdot 10^{-1}$ for the faulty motor.

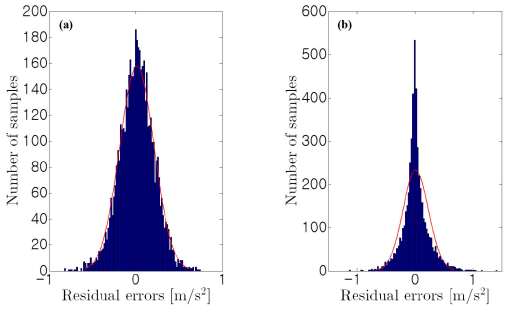

FIGURE 13. Results of fitting the histogram of the AKF residuals to a normal distribution: (a) healthy motor and (b) faulty motor.

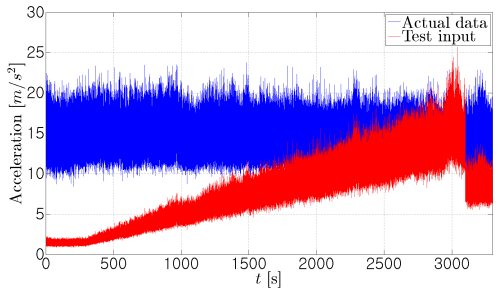

FIGURE 14. Test inputs for demonstrating the availability of the proposed CM.

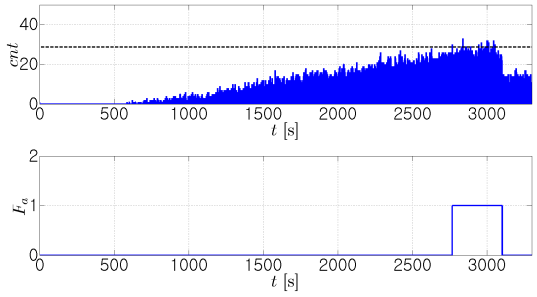

FIGURE 15. Outlier and failure detection results for the test input.

estimates of healthy motor are bounded to the adaptive upper and lower thresholds. In contrast, the estimates of the faulty motor are more frequently shown to deviate from the range of the adaptive thresholds. For both cases, the residual errors of AKF are bounded between reasonably small values and distributed with almost zero mean thanks to the adaptation law. Figure 13 shows the results of fitting a histogram of 5000 residual error samples to a normal distribution, demonstrating the validity of the zero-mean Gaussian assumption for deriving (11) used to estimate $Q(k)$.

To demonstrate the availability of the proposed failure detection and CM techniques, test input is created based on the collected data from the faulty motor, as shown in Figure 14. Figure 15 shows the outlier detection and failure detection results for the AKF_{10}. The number of outliers detected per second increased as the test input evolves, reaching the value f_r for the first time at 2683s. At this time, the motor failure is detected. Figure 16 shows the severity assessment results of the test input. It can be seen that an AKF with a larger $R(k)$ contributes to detecting more severe anomaly condition. The result after 3100s shows that the severity index can decrease as the vibration severity of the IM decreases.

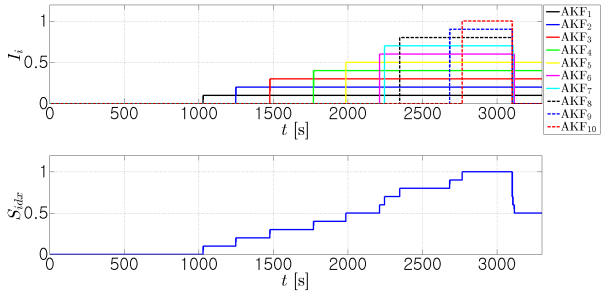

FIGURE 16. Severity assessment for the test input.

In real-world applications where it is not known when a failure occurs, the proposed severity assessment method can be used for early failure detection and efficient maintenance, considering a severity index criterion of less than 1.

V. CONCLUSION

In this paper, a cost-effective CM technique using a single accelerometer to support the condition-based maintenance of IMs has been proposed. The proposed methodology is based on an AKF and includes outlier classification, anomaly detection, and severity assessment steps. In this study, to develop the AKF-based CM technique, valuable discussions were made with the aim of improving the convergence property of Kalman filters, setting adaptive thresholds for outlier classification, and detecting anomalies and failures. Furthermore, the motor's condition was assessed using multiple AKFs. Although the proposed CM technique could not identify different types of faults, it could be used for the early detection of failures without requiring well-defined knowledge of the dynamic models and fault types of IMs. The applicability of the proposed CM strategy was demonstrated through a set of experiments using real scrubber fan systems.

REFERENCES

[1] X. Liang and K. Edomwandekhoe, "Condition monitoring techniques for induction motors," in *Proc. IEEE Ind. Appl. Soc. Annu. Meeting*, Oct. 2017, pp. 1–10.

[2] M. R. Barusu and M. Deivasigamani, "Non-invasive vibration measurement for diagnosis of bearing faults in 3-phase squirrel cage induction motor using microwave sensor," *IEEE Sensors J.*, vol. 21, no. 2, pp. 1026–1039, Jan. 2021.

[3] J. Martinez, A. Belahcen, and A. Muetze, "Analysis of the vibration magnitude of an induction motor with different numbers of broken bars," *IEEE Trans. Ind. Appl.*, vol. 53, no. 3, pp. 2711–2720, May 2017.

[4] A. Giantomassi, F. Ferracuti, S. Iarlori, G. Ippoliti, and S. Longhi, "Electric motor fault detection and diagnosis by kernel density estimation and Kullback–Leibler divergence based on stator current measurements," *IEEE Trans. Ind. Electron.*, vol. 62, no. 3, pp. 1770–1780, Mar. 2015.

[5] S. Hemamalini, "Rational-dilation wavelet transform based torque estimation from acoustic signals for fault diagnosis in a three-phase induction motor," *IEEE Trans. Ind. Informat.*, vol. 15, no. 6, pp. 3492–3501, Jun. 2019.

[6] A. Choudhary, D. Goyal, and S. S. Letha, "Infrared thermography-based fault diagnosis of induction motor bearings using machine learning," *IEEE Sensors J.*, vol. 21, no. 2, pp. 1727–1734, Jan. 2021.

[7] Y. Hu, W. Bao, X. Tu, F. Li, and K. Li, "An adaptive spectral kurtosis method and its application to fault detection of rolling element bearings," *IEEE Trans. Instrum. Meas.*, vol. 69, no. 3, pp. 739–750, Mar. 2020.

[8] Z. Zhang, Y. Wang, and K. Wang, "Fault diagnosis and prognosis using wavelet packet decomposition, Fourier transform and artificial neural network," *J. Intell. Manuf.*, vol. 24, no. 6, pp. 1213–1227, Dec. 2013.

[9] G. R. Agah, A. Rahideh, H. Khodadadzadeh, S. M. Khoshnazar, and S. Hedayatikia, "Broken rotor bar and rotor eccentricity fault detection in induction motors using a combination of discrete wavelet transform and Teager–Kaiser energy operator," *IEEE Trans. Energy Convers.*, vol. 37, no. 3, pp. 2199–2206, Sep. 2022.

[10] L. A. Trujillo-Guajardo, J. Rodriguez-Maldonado, M. A. Moonem, and M. A. Platas-Garza, "A multiresolution Taylor–Kalman approach for broken rotor bar detection in cage induction motors," *IEEE Trans. Instrum. Meas.*, vol. 67, no. 6, pp. 1317–1328, Jun. 2018.

[11] F. Dalvand, A. Kalantar, and M. S. Safizadeh, "A novel bearing condition monitoring method in induction motors based on instantaneous frequency of motor voltage," *IEEE Trans. Ind. Electron.*, vol. 63, no. 1, pp. 364–376, Jan. 2016.

[12] S. Zhang, S. Zhang, B. Wang, and T. G. Habetler, "Deep learning algorithms for bearing fault diagnostics—A comprehensive review," *IEEE Access*, vol. 8, pp. 29857–29881, 2020.

[13] D. T. Hoang and H. J. Kang, "A motor current signal-based bearing fault diagnosis using deep learning and information fusion," *IEEE Trans. Instrum. Meas.*, vol. 69, no. 6, pp. 3325–3333, Jun. 2020.

[14] A. K. Verma, S. Nagpal, A. Desai, and R. Sudha, "An efficient neural-network model for real-time fault detection in industrial machine," *Neural Comput. Appl.*, vol. 33, no. 4, pp. 1297–1310, Feb. 2021.

[15] M. Z. Ali, M. N. S. K. Shabbir, X. Liang, Y. Zhang, and T. Hu, "Machine learning-based fault diagnosis for single- and multi-faults in induction motors using measured stator currents and vibration signals," *IEEE Trans. Ind. Appl.*, vol. 55, no. 3, pp. 2378–2391, May 2019.

[16] J. Wang, P. Fu, L. Zhang, R. X. Gao, and R. Zhao, "Multilevel information fusion for induction motor fault diagnosis," *IEEE/ASME Trans. Mechatronics*, vol. 24, no. 5, pp. 2139–2150, Oct. 2019.

[17] M. D. Prieto, G. Cirrincione, A. G. Espinosa, J. A. Ortega, and H. Henao, "Bearing fault detection by a novel condition-monitoring scheme based on statistical-time features and neural networks," *IEEE Trans. Ind. Electron.*, vol. 60, no. 8, pp. 3398–3407, Aug. 2013.

[18] H. Su and K. T. Chong, "Induction machine condition monitoring using neural network modeling," *IEEE Trans. Ind. Electron.*, vol. 54, no. 1, pp. 241–249, Feb. 2007.

[19] F. Ben Abid, S. Zgarni, and A. Braham, "Distinct bearing faults detection in induction motor by a hybrid optimized SWPT and aiNet-DAG SVM," *IEEE Trans. Energy Convers.*, vol. 33, no. 4, pp. 1692–1699, Dec. 2018.

[20] M. He and D. He, "Deep learning based approach for bearing fault diagnosis," *IEEE Trans. Ind. Appl.*, vol. 53, no. 3, pp. 3057–3065, May 2017.

[21] S. E. Pandarakone, Y. Mizuno, and H. Nakamura, "Distinct fault analysis of induction motor bearing using frequency spectrum determination and support vector machine," *IEEE Trans. Ind. Appl.*, vol. 53, no. 3, pp. 3049–3056, May 2017.

[22] J. Zarei, E. Kowsari, and R. Razavi-Far, "Induction motors fault detection using square-root transformed cubature quadrature Kalman filter," *IEEE Trans. Energy Convers.*, vol. 34, no. 2, pp. 870–877, Jun. 2019.

[23] B.-G. Gu, "Study of IPMSM interturn faults—Part II: Online fault parameter estimation," *IEEE Trans. Power Electron.*, vol. 31, no. 10, pp. 7214–7223, Oct. 2016.

[24] S. Bachir, S. Tnani, J.-C. Trigeassou, and G. Champenois, "Diagnosis by parameter estimation of stator and rotor faults occurring in induction machines," *IEEE Trans. Ind. Electron.*, vol. 53, no. 3, pp. 963–973, Jun. 2006.

[25] Y.-H. Kim, Y.-W. Youn, D.-H. Hwang, J.-H. Sun, and D.-S. Kang, "High-resolution parameter estimation method to identify broken rotor bar faults in induction motors," *IEEE Trans. Ind. Electron.*, vol. 60, no. 9, pp. 4103–4117, Sep. 2013.

[26] M. F. Tariq, A. Q. Khan, M. Abid, and G. Mustafa, "Data-driven robust fault detection and isolation of three-phase induction motor," *IEEE Trans. Ind. Electron.*, vol. 66, no. 6, pp. 4707–4715, Jun. 2019.

[27] F. Duan and R. Zivanovic, "Condition monitoring of an induction motor stator windings via global optimization based on the hyperbolic cross points," *IEEE Trans. Ind. Electron.*, vol. 62, no. 3, pp. 1826–1834, Mar. 2015.

[28] V. Climente-Alarcon, J. A. Antonino-Daviu, E. G. Strangas, and M. Riera-Guasp, "Rotor-bar breakage mechanism and prognosis in an induction motor," *IEEE Trans. Ind. Electron.*, vol. 62, no. 3, pp. 1814–1825, Mar. 2015.

[29] D. Z. Li, W. Wang, and F. Ismail, "A spectrum synch technique for induction motor health condition monitoring," *IEEE Trans. Energy Convers.*, vol. 30, no. 4, pp. 1348–1355, Dec. 2015.
[30] X. Jin, Z. Que, Y. Sun, Y. Guo, and W. Qiao, "A data-driven approach for bearing fault prognostics," *IEEE Trans. Ind. Appl.*, vol. 55, no. 4, pp. 3394–3401, Jul. 2019.
[31] M. Kordestani, M. Saif, M. E. Orchard, R. Razavi-Far, and K. Khorasani, "Failure prognosis and applications—A survey of recent literature," *IEEE Trans. Rel.*, vol. 70, no. 2, pp. 728–748, Jun. 2021.
[32] D. Z. Li, W. Wang, and F. Ismail, "An enhanced bispectrum technique with auxiliary frequency injection for induction motor health condition monitoring," *IEEE Trans. Instrum. Meas.*, vol. 67, no. 10, pp. 2679–2687, Oct. 2015.
[33] S. Kumar, D. Mukherjee, P. K. Guchhait, R. Banerjee, A. K. Srivastava, D. N. Vishwakarma, and R. K. Saket, "A comprehensive review of condition based prognostic maintenance (CBPM) for induction motor," *IEEE Access*, vol. 7, pp. 90690–90704, 2019.
[34] W. Ahmad, S. A. Khan, and J.-M. Kim, "A hybrid prognostics technique for rolling element bearings using adaptive predictive models," *IEEE Trans. Ind. Electron.*, vol. 65, no. 2, pp. 1577–1584, Feb. 2018.
[35] S. Badoni and R. K. Jarial, "Health monitoring of three phase induction motor using infrared thermography," in *Proc. 6th Int. Conf. Commun. Electron. Syst. (ICCES)*, Jul. 2021, pp. 156–160.
[36] L. Cui, X. Wang, Y. Xu, H. Jiang, and J. Zhou, "A novel switching unscented Kalman filter method for remaining useful life prediction of rolling bearing," *Measurement*, vol. 135, pp. 678–684, Mar. 2019.
[37] F. Yang, M. S. Habibullah, T. Zhang, Z. Xu, P. Lim, and S. Nadarajan, "Health index-based prognostics for remaining useful life predictions in electrical machines," *IEEE Trans. Ind. Electron.*, vol. 63, no. 4, pp. 2633–2644, Apr. 2016.
[38] Y. Qian, R. Yan, and S. Hu, "Bearing degradation evaluation using recurrence quantification analysis and Kalman filter," *IEEE Trans. Instrum. Meas.*, vol. 63, no. 11, pp. 2599–2610, Nov. 2014.
[39] R. K. Singleton, E. G. Strangas, and S. Aviyente, "Extended Kalman filtering for remaining-useful-life estimation of bearings," *IEEE Trans. Ind. Electron.*, vol. 62, no. 3, pp. 1781–1790, Mar. 2015.
[40] X. Jin, Y. Sun, Z. Que, Y. Wang, and T. W. S. Chow, "Anomaly detection and fault prognosis for bearings," *IEEE Trans. Instrum. Meas.*, vol. 65, no. 9, pp. 2046–2054, Sep. 2016.
[41] P. N. Phuc, D. Bozalakov, H. Vansompel, K. Stockman, and G. Crevecoeur, "Rotor temperature virtual sensing for induction machines using a lumped-parameter thermal network and dual Kalman filtering," *IEEE Trans. Energy Convers.*, vol. 36, no. 3, pp. 1688–1699, Sep. 2021.
[42] A. K. Samanta, A. Routray, S. R. Khare, and A. Naha, "Minimum distance-based detection of incipient induction motor faults using Rayleigh quotient spectrum of conditioned vibration signal," *IEEE Trans. Instrum. Meas.*, vol. 70, pp. 1–11, 2021.
[43] J. Kim, B. Kiss, D. Kim, and D. Lee, "Tracking control of overhead crane using output feedback with adaptive unscented Kalman filter and condition-based selective scaling," *IEEE Access*, vol. 9, pp. 108628–108639, 2021.
[44] J. Kim, D. Lee, B. Kiss, and D. Kim, "An adaptive unscented Kalman filter with selective scaling (AUKF-SS) for overhead cranes," *IEEE Trans. Ind. Electron.*, vol. 68, no. 7, pp. 6131–6140, Jul. 2021.

JAEHOON KIM received the B.S. and M.S. degrees in electronics engineering and the Ph.D. degree in electronic and electrical engineering from Kyungpook National University, Daegu, South Korea, in 2011, 2013, and 2021, respectively. Since 2020, he has been a Lecturer with the College of Information and Communication Engineering, Daegu University, Gyeongsan, South Korea. He is currently a Postdoctoral Research Fellow with the Institute of Electronic Technology, Kyungpook National University. His current research interests include nonlinear estimation and filtering, control engineering, and monitoring and diagnostic techniques.

MOOGEUN SONG received the B.S. and M.S. degrees in electronics engineering from Kyungpook National University, Daegu, South Korea, in 2008 and 2010, respectively, where he is currently pursuing the Ph.D. degree. Since 2017, he has been a Lecturer with the School of Computer Aided Mechanical Engineering, Yungjin University, Deagu. His current research interests include fieldbus networks, fault-tolerant system embedded systems, and formal verification.

DONGGIL KIM received the B.Sc., M.Sc., and Ph.D. degrees in electronics engineering from Kyungpook National University, Daegu, South Korea, in 2006, 2008, and 2015, respectively. Since 2017, he has been with the Department of Robot Engineering, Kyungil University, Gyeongsan, South Korea, where he is currently an Assistant Professor. From 2015 to 2017, he was a Senior Researcher with the Defense Agency for Technology and Quality, South Korea. His current research interests include fault tolerant control, fault detection and diagnosis, and fieldbus for the design of dependable networked control systems.

DONGIK LEE (Member, IEEE) received the B.S. and M.S. degrees in control engineering from Kyungpook National University, Daegu, South Korea, in 1987 and 1990, respectively, and the Ph.D. degree in complex systems control engineering from Sheffield University, Sheffield, U.K., in 2002.

He is currently a Professor with the School of Electronic and Electrical Engineering, Kyungpook National University. His research interests include the design of real-time networked control for various safety-critical applications, including autonomous underwater vehicles, wind turbines, and intelligent automobiles.